Molecular Dynamics Simulation of Sphingomyelin Bilayer

Marja T. Hyvönen*,†,‡ and Petri T. Kovanen†

Wihuri Research Institute, Kalliolinnantie 4, 00140 Helsinki, Finland and Laboratory of Physics and Helsinki Institute of Physics, Helsinki University of Technology, P.O. Box 1100, FIN-02015, HUT, Finland

Received: May 13, 2003

Besides phosphatidylcholines and cholesterol, sphingomyelin molecules are the most important lipid species in the biological membranes, and their role has recently been emphasized in various membrane phenomena, such as domain formation. Here, a multinanosecond molecular dynamics (MD) simulation study was performed at physiological temperature for a hydrated bilayer system, consisting of 128 palmitoylsphingomyelin (16:0-SM) molecules. Analysis of the structural parameters of the system indicates that 16:0-SM bilayer is in a mixed state of liquid-crystalline and condensed phases, which results in considerable ordering in the hydrocarbon chain region. The simulation also revealed major differences in the hydrogen-bonding properties between the sphingomyelin and phosphatidylcholine molecules. In the future, MD simulation studies are also likely to shed light on the detailed structural properties of the lateral membrane domains of mammalian cells, termed rafts, which form because of association of sphingolipids and cholesterol.

Introduction

In all eukaryotic cell membranes and other membrane structures, such as the surface of lipoproteins, sphingomyelin (SM) molecules together with phosphatidylcholine and cholesterol molecules, are crucial. In addition to their role as biomembrane constituents, the metabolic derivatives of SM are involved in cell signaling. Thus, sphingosine, the basis of sphingolipids, mediates cell proliferation,[1,2] and ceramide, the product of hydrolysis by sphingomyelinase, serves as a second messenger for the stimulation of kinases and phosphatases, which regulate cell growth and apoptosis.[1]

Phosphatidylcholine (PC) molecules, the most common glycerophospholipids, share several features in common with SM: both have similar phosphocholine as zwitterionic polar headgroup and two long fatty acyl chains.[3] Although these chains have even been reported to have a similar relative conformation in their first segments,[4] the differences in the fatty acid composition are significant, since the naturally occurring SMs are, on average, highly saturated as compared with the naturally occurring PCs. Moreover, the sphingosine backbone structure in SM, instead of the glycerol backbone in PC, results in extra hydrogen-bonding properties at the water−membrane interface.[3,4]

The molecular differences between PCs and SMs have been found to result in their different abilities to interact with cholesterol.[3,4] Thus, preferential interaction between SM and cholesterol has been postulated to be a driving force in the formation of lateral domains in biomembranes. In mammalian cells, these domains, which are termed rafts, have been suggested to be involved in the lateral recruitment of certain types of proteins.[5,6] Interestingly, differences in the mobility of PC and SM headgroups have also been observed in the surface layer of low-density lipoprotein.[7] The differences in the behavior of PCs and SMs have also been suggested to result in domain formation in these highly specialized particles of lipid transport.[7,8]

The interaction of SM with cholesterol and other lipid constituents has been widely studied[9] and some interest in the structural properties of SM molecules at the molecular level has risen.[3,10−14] Still, the amount of information on SM is surprisingly moderate as compared with PC molecules. Molecular dynamics (MD) simulations are able to provide information on molecular level characteristics of lipid systems and the number of such studies has been steadily increasing in recent years.[15−20] However, in the past SM molecules have not been incorporated to the MD simulations of biomolecular systems. During the referee process of this paper, an MD simulation study on SM bilayer has been published.[21] The intention to raise computational methods as a relevant tool for studying the molecular level phenomena in biological membranes requires that all major lipid components are considered in computational studies. The SM studied here contains sphingosine (18:1) as a long-chain base and palmitic acid (16:0) as a fatty acid. These components comprise a total of 93% and ∼70% of natural egg SM,[22] and the 16:0 chain has been found in significant proportions also in, for example, normal human skin fibroblasts.[22] A fully hydrated bilayer of 128 16:0-SM molecules was simulated to obtain detailed information on the structure of the headgroup, backbone, and chain regions of these molecules. Special emphasis is given for the analysis of the interactions of the hydrogen-bonding groups and the ordering of the hydrocarbon chains.

Methods

Modeling and Computational Details. The SM molecule used to construct the bilayer model is shown in Figure 1. The molecule (16:0-SM) in the present study consists of 18:1-sphingosine (SPH) as the long-chain base and 16:0-palmitic acid (PA) as the fatty acid. The molecule was built by utilizing both the Dundee PRODRG Server[23] and Insight software.[24] The PRODRG service was used only to get an initial structure, which

* Corresponding author. Tel.: +358−9−681 4132; fax: +358−9−637 476; e-mail: Marja.Hyvonen@wri.fi.
† Wihuri Research Institute.
‡ Helsinki University of Technology.

10.1021/jp035319v CCC: $25.00
Published on Web 07/24/2003

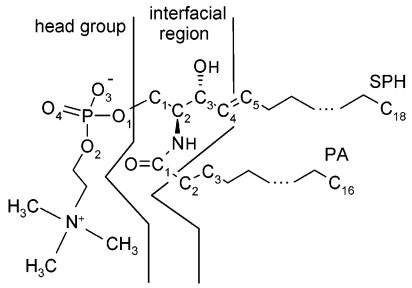

Figure 1. Molecular structure of 16:0-SM molecule indicating the naming of molecular groups and the atom numbering.

was then modified to account for the known details of SM molecules. Since the biophysical properties of the stereochemically different *erythro* and *threo* forms differ significantly,[12] special care was taken to build the physiologically relevant D-*erythro*-sphingomyelin. The energy of a single 16:0-SM was minimized and the molecule was copied and rotated around its long axis to form a block of four molecules in a squarelike configuration with approximately 8 Å separations. The long axis of the molecules was aligned along the *y*-axis of the system and the energy of the system was minimized. The block was copied in the $x-z$ plane to form a squarelike monolayer of 64 16:0-SM molecules, of which the energy was again minimized. The monolayer was duplicated to form a bilayer of 128 16:0-SM molecules. The energy of the pure lipid system was minimized and the system was simulated in the NVE ensemble with the area per lipid of 64 Å^2 for 80 ps, keeping the phosphorus atoms fixed, to allow the chains of the molecules to relax. The hydration of the system was performed utilizing pre-equilibrated box of 125 TIP3P water molecules (available in CHARMM software).[25] The small box of water was copied to form a box of 2000 water molecules with dimensions of 62.2 $\times$ 15.55 $\times$ 62.2 Å^3, the energy of the large box was minimized, and water boxes were placed on both sides of the lipid bilayer. The 128-molecule piece of the bilayer, together with 4000 water molecules, was used to model an infinite bilayer by applying periodic boundary conditions. The final energy minimization was reached by stabilizing first the water molecules and then the whole system. The total number of atoms in the system was 28 256. After the energy minimization of the system, the first equilibration simulation of the whole system was started at a temperature of 37 °C (310 K) with the a time step of 1.0 fs. This simulation lasted for 110 ps, after which the energy was again minimized. The initial equilibration runs ensured disordering of the system to minimize the effect of initial construction to the final production simulation. Thereafter, a 2-ns simulation was initiated, using the leapfrog verlet algorithm with a time step of 1.0 fs. Thereafter, again, the energy of the system was minimized and a new simulation initiated with a time step of 1.2 fs, to speed up the simulation. The temperature, the energy components, and the dimensions of the systems were monitored during the simulation to ensure their stability and the adequacy of the length of the period for collecting the data for analysis. This last phase of the simulation lasted for 3.4 ns and the data from the last 1 ns was used to analyze the membrane properties reported here. The simulations were performed in an NPT ensemble to maintain temperature of 310 K and isotropic pressure of 1 atm with a Nose−Hoover thermostat and a Langevin piston, except in the early equilibration run for the lipid bilayer alone (as mentioned above). The piston collision frequency was 5 ps^{-1} and the masses of the pressure and thermal pistons were 500 amu and 1000 kcalps^2, respectively. The evolution of the average area per lipid is shown in Figure 2. The primary model system is shown in Figure 3 as a snapshot both from the early state of the equilibration (at 600 ps) and from the end of the simulation. These figures clearly show that the considerable amount of order in the equilibrated structure was not due to the way the system was constructed but arose during equilibration.

The simulation was performed, applying the CHARMM software (CHARMM Ver. 27).[25] Mostly, lipid force field parameters were used.[26] As SM was not included in the CHARMM force field, the parameters for the middle part of the molecule, where the "nitrogen linkage" is located, were taken from the parameters of CHARMM protein force field. The force field of the SM molecule is available as the Supporting Information. For water molecules, the TIP3P parameters[27] were used. All the atoms were taken into account independently in the MD simulation. The lengths of the bonds involving hydrogen atoms were fixed using the SHAKE algorithm. Electrostatic interactions were included via the particle mesh Ewald summation,[28,29] with grid size of 64 $\times$ 64 $\times$ 64. The Lennard-Jones potential was switched to zero in the region from 10 to 12 Å. The nonbonded interactions were updated every 10th step, which was enough to maintain constant energy. Energies, coordinates, and velocities were saved every 50th step.

Data Analysis. In the subsequent analysis, the averages have been calculated over every second of saved time steps of production run (last 1 ns) and over all lipid or water molecules, if not otherwise stated. Also, the properties in the bilayer normal direction are averaged over both leaflets, considering the middle of the simulation box as $y = 0$.

Single atomic distribution functions in the bilayer normal direction were evaluated by calculating the total number of each type of atom in 0.25 Å thick slices. The distributions were averaged over time. Further, they were used to calculate the electron density across the bilayer. Various radial distribution functions (RDFs) were calculated using the gOpenMol software.[30] The RDFs were averages of two distinct periods from the last 1 ns of the simulation, to ensure that the RDFs would characterize the interactions during the production period and not only part of it. The time periods were 54 and 55 ps from the beginning and at the end of the last 1 ns, respectively. The mean cosine of the angle between the water dipole moment vector and the bilayer normal in 0.25 Å slices along the bilayer normal was also calculated. A zero value is obtained for a random orientation and a positive value corresponds to the orientation of the dipole toward the bilayer center. The orientation angles of the headgroup phosphorus−nitrogen vector and various carbon−carbon vectors with respect to the bilayer normal, as well as the angle distributions, were determined using one degree slices.

The electrostatic potential profile along the bilayer normal *y* was calculated on the basis of Poisson's equation:

$$\psi(y) - \psi(0) = -\frac{1}{\epsilon_0}\int_0^y \int_0^{y'} \rho(y'')dy''dy'$$

where $\psi(y)$ is the electrostatic potential, $\rho(y)$ is the charge density at *y*, and ϵ_0 is the vacuum permittivity. The charge density was determined in 0.25 Å thick slices and averaged from the monolayers. The position $y = 0$ resides in the middle of the bilayer.

The orientational order is described by the order parameter S_j, which is defined as

$$S_j = \frac{1}{2}\langle 3\cos^2\beta_j - 1\rangle, \qquad (1)$$

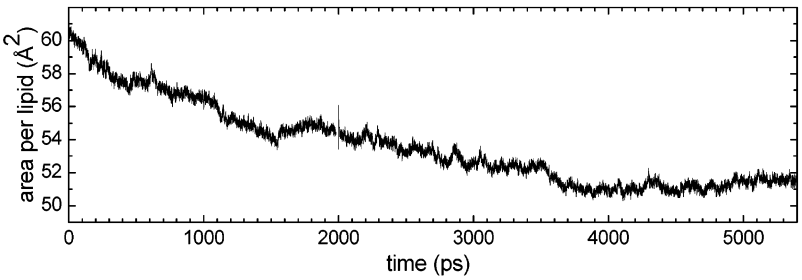

Figure 2. Time course of the area per lipid during simulation. Only the last 1 ns was utilized in the analysis of the average properties reported here.

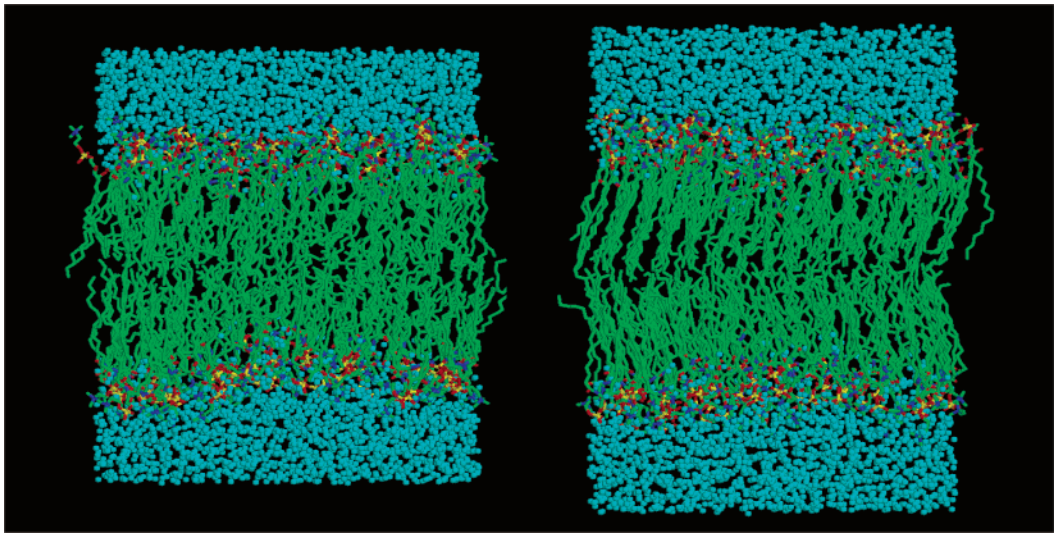

Figure 3. Snapshot of the primary simulation box at the beginning (left) and at the end (right) of the total simulation. The simulation was started with liquid-crystalline-like properties of the chain region and ended up with a mixed state of condensed and liquid-crystalline states, consistent with the experiments.[13] Water molecules are shown in cyan, and the color coding of the lipid molecules is as follows: green for carbon, red for oxygen, yellow for phosphorus, and blue for nitrogen. For clarity, the hydrogen atoms are not shown. The *y* axis is normal to the membrane.

where β_j is the angle between the orientation vector and the reference direction. The brackets denote both the ensemble and time average. A ^{2}H NMR observable order parameter, S_j^{CD}, is obtained by defining the orientation vector along the CH_j bond, with the bilayer normal as the reference direction. According to this definition, we calculated the order parameters for the two CH bonds, CH_{aj} and CH_{bj}, at each saturated carbon atom in the chains. As an error estimation, the standard error of the mean (SEM) of the 128 molecular averages is given. For each of the molecules, the molecular average was evaluated from the whole time series of 1 ns. In this way, the effect of high correlation between consecutive time steps is eliminated, which results in more realistic error estimates. According to the conventional way in MD simulations, the orientation vector is often defined along the normal of the HC_jH plane or from C_{j-1} to C_{j+1}, which leads to the molecular order parameter S_j^{mol}. When isotropic rotations around the HC_jH plane normal are assumed, the CH bonds and corresponding S_j^{CD} values become equivalent, and S_j^{CD} can be compared with the S_j^{mol} values according to the relation $-2S_j^{CD} = S_j^{mol}$.[31] The S_j^{mol} may vary between $-1/2$ and 1 corresponding to the variation between perpendicular (90 degrees) and parallel (0 degrees) orientation with respect to the bilayer normal. Usually, the zero value of S_j indicates isotropic orientation distribution but, for example, a single orientation angle of 54.7° in the sample also results in the zero value.

Results and Discussion

The time course of the average area per 16:0-SM molecule during the equilibration and the production run is presented in Figure 2. During the last nanoseconds, the average area per lipid has equilibrated, giving the average value of 51.5 Å^2 for the last 1 ns. To the best of our knowledge, measurements of the area per lipid for a bilayer system at physiological temperature are lacking, but values of 47.4 and 52.5 Å^2 have been reported at the temperatures of 24 and 30 °C, on the basis of measurements using the Langmuir film balance at the surface pressure of 30 mN/m.[13] On the other hand, measurements based on X-ray diffraction with varying hydration suggest values of 41 and 47 Å^2 at the temperatures of 29 and 55 °C.[11] Therefore, keeping in mind the experimental difficulties, the possible effect of the utilization of racemic SMs,[12] and that monolayers and bilayers are not necessarily directly comparable, reasonable agreement with the experimental predictions is achieved. The transition temperature between the liquid and condensed phases has been reported to be 41.1 °C or 40.5 °C for this particular SM,[12,13] and at 30 °C the system is reported to behave as a mixed state of both liquid and condensed phases.[13] The visual observation of the bilayer system at the beginning of the equilibration and at the end of the simulation in Figure 3 shows that at this time scale and at physiological temperature, the system has equilibrated to a mixed state, where part of the chains are prone to cooperative order, without this phenomenon being strong enough to lead to ordering of the whole system. Figure 3 also shows that the features of condensed phase, that is, the ordering and cooperative tilt of the chains, did not exist at the start but appeared later reflecting an equilibrated state of the membrane. Interestingly, experimental studies have indicated complex phase behavior for the sphingomyelin systems, as, for instance, four distinct gel phases have been found in 18:0-SM systems.[32]

According to the experimental studies on purely gel-phase-saturated phosphatidylcholine molecules, the tilt has been shown to be such that the direction of the chains in opposing leaflets is parallel to each other whereas with 90 degrees rotation in the plane of the membrane, there should not be pleated structure observable in the chains.[33,34] This kind of structure has also been produced by careful simulations of Venable et al.[35] Here, no pure gel phase is seen (and not expected on the basis of the experimental studies on this particular sphingomyelin[13]), but partial ordering of the system looks like a "herringbone" structure. However, we cannot exclude such local type of ordering in these mixed state systems on the basis of experiments on PC in a pure gel phase.

The atomic distributions in the bilayer normal direction are shown in Figure 4. The width of the distributions reveals a considerable amount of roughness in the bilayer surface. The water molecules are able to penetrate as far as C5 of the sphingosine. The motional freedom in the bilayer normal direction in the bilayer surface is of the same order as in liquid-crystalline palmitoyllinoleoylphosphatidylcholine (PLPC).[36] However, the chains show restricted motion as compared with liquid-crystalline PLPC: for the PLPC, the height of the distributions steadily decreases toward the bilayer center, indicating increasing motional freedom, whereas, in 16:0-SM, even an increase in the peak height is seen. Interestingly, despite the ordered nature of this system at the physiological temperature, there is a small but definite amount of overlap between the distributions of the methyl carbons C16 and C18 and the water region. This points to the possible importance of rare local structures and events in systems of this kind. For instance, although the general ordered structure of the system seems incompatible with any penetration of water molecules, the penetration is known to take place.[37] Within the time scales of the present MD simulations, such a phenomenon is not observed, but the rare local disturbances observed give a hint that, owing to the suitable availability of free volume because of such local disturbances, the water molecule might be able to penetrate further inside the membrane. During the equilibrium state of the simulation, the average phosphorus−phosphorus distance is 44.2 Å, whereas 49.6 Å and 44.4 Å have been reported on the basis of the X-ray measurements at 29 °C and 55 °C.[11]

Figure 4 also presents the electron density profile along the bilayer normal, together with the approximate best-fit electron densities of a three-slab model presented by Vaknin et al. for C18−SM.[38] Comparison of the simulation-based profile with the X-ray reflectivity based results shows good agreement and gives further support for the simulation results in general.

Furthermore, the orientational behavior of the water molecules and the electrostatic potential across the membrane are shown in Figure 4. The orientational behavior of the water molecules is here described as the mean cosine of the angle between the water dipole moment vector and the bilayer normal. Similarly to the PC systems, the positive peak in the region of the headgroups is due to the strong orientation of the hydrogen atoms of the water molecules toward the phosphorus atoms,[36] which is clearly seen in the radial distribution functions (RDFs) in Figure 5. At the interfacial region of approximately 10−19 Å, the OH and NH groups of the SM molecules cause extra orientation of the water molecules as compared with the PCs. The negativity of the profile in this region is due to the dominating orientation of the water dipole toward the water phase, with the oxygen atoms of the water molecules pointing toward the OH and NH groups of 16:0-SM molecules, as can be seen in the RDFs in Figure 5 and will be discussed below.

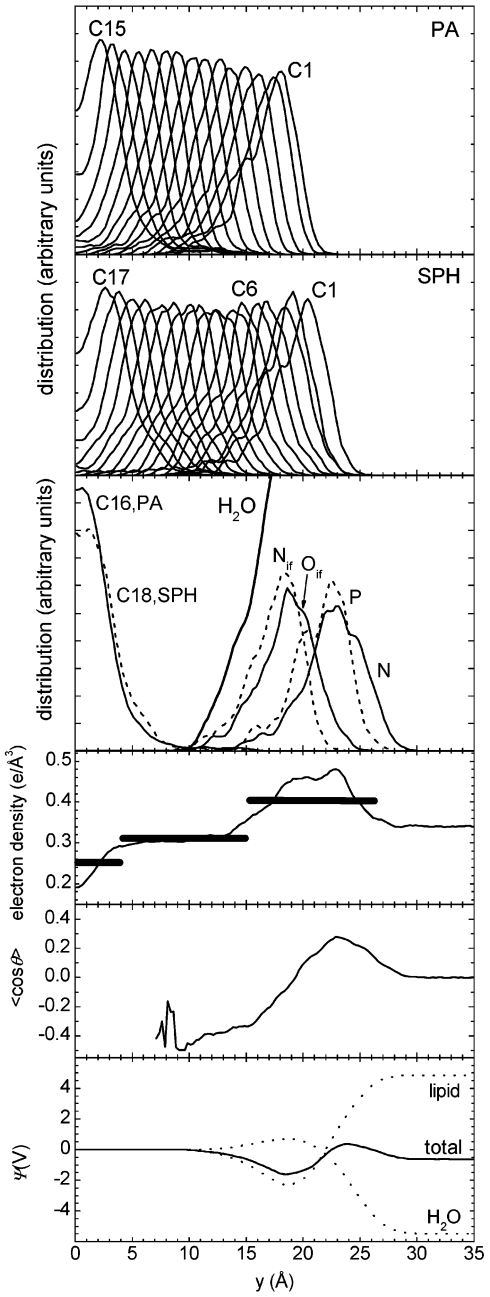

Figure 4. Atomic distribution functions (three upper panels) of palmitoyl chain carbon atoms (PA), sphingosine carbon atoms (SPH), and water oxygen atoms (H_2O) together with the headgroup phosphorus (P) and nitrogen (N), and with the interfacial region nitrogen (N_{if}) and oxygen (O_{if}) of the NH and OH groups. These distributions are given in similar units. In addition, the electron density profile, the orientation of the water molecules with respect to the bilayer normal, and the electrostatic potential are shown along the bilayer normal (three lower panels). In all panels, the averaging has been performed over both layers. The electron density profile is compared with the three-slab density model based on the X-ray data.[38] In the lowest panel, the contributions of lipid and water molecules are given separately together with the total potential.

The electrostatic potential profile along the bilayer normal was calculated together with the separate contributions from the lipids and water, and the profiles are shown in the lowest panel of Figure 4. The total potential is negative in the water region as compared with the interior of the bilayer, with the value of the potential of −0.63 V. As in PC membranes,[39−41] the contribution of lipids is several volts. This is overcompensated by the orientation of the water molecules, which results

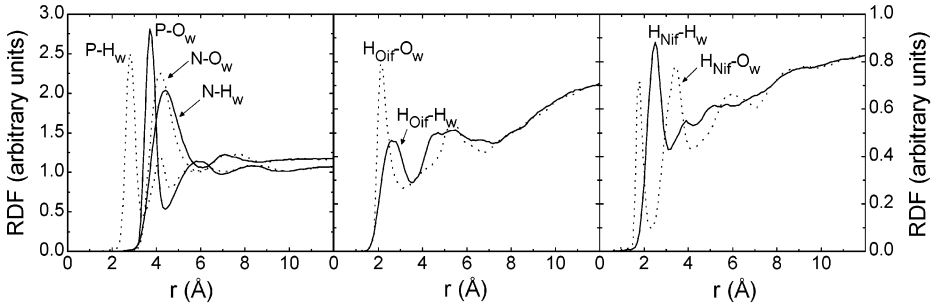

Figure 5. Radial distributions of the oxygen (O_w, dashed line) and hydrogen (H_w, solid line) atoms of water molecules around the phosphorus (P) and nitrogen (N) atoms of the headgroups (left) and around the hydrogen atoms of the OH group (H_{Oif}, middle) and the NH group (H_{Nif}, right) of the interfacial region. The middle and right panels have the same scale, differing from the left panel.

in the negative total potential in the water region as compared with the interior of the bilayer. The experimental values for the potential range from −200 mV to −575 mV for different phospholipid/water interfaces.[42−45]

The average orientation angle of the phosphorus−nitrogen vector of the 16:0-SM headgroups with respect to the bilayer plane was 16.7° and the distribution of angles was from −50° to +90° (the negative angle corresponds to orientations toward the bilayer center). Therefore, the average orientation and mobility do not significantly differ from what has been reported for the PCs on the basis of experiments and simulations.[36,46]

Various radial distribution functions (RDFs) were calculated between the possibly water-orienting groups of SM and water and are shown in Figure 5. Although the RDFs were calculated until $r = 20$ Å, the profiles were practically featureless after 10 Å, and therefore the RDFs shown here range only to 10−12 Å. First, the orientational behavior of the water molecules around the phosphatidyl and choline groups were defined. The water molecules were strongly oriented around the phosphorus atom because of the hydrogen bonding between the oxygen atoms of the phosphatidyl group and the hydrogen atoms of the water molecules. Only a weak orientation is noticed around the nitrogen atom, most likely because of the hydrophobic nature of the surrounding methyl groups, which results in hydrogen bonding among the water molecules. A very similar arrangement of water molecules around the PC headgroups has also been observed in other MD simulation studies of PC systems.[36,47−49] The properties of the interfacial region of the SMs are distinct from those in the PCs because of the extra hydrogen-bonding properties of the NH and OH groups. Figure 5 also reveals the hydrogen bonding of water molecules to the NH and OH groups. It has been suggested that hydrogen bonding to water is involved in the formation of the water bridges between the SM molecules,[14] which possibility is supported by the RDFs of Figure 5.

Figure 6 shows the radial distribution functions of potential lipid−lipid hydrogen-bonding partners in this region. Both the NH group and OH group are able to closely interact with the phosphatidyl oxygens. Figure 7 shows two snapshots of the conformations, which lead to the largest peaks in the RDFs in Figure 6. As the RDF reveals, the NH group is mostly near the $O1_P$, although one cannot define hydrogen bonding between them, as the angle does not fulfill the criteria for the hydrogen bonding. However, the existence of RDF already at 2.5 Å for the other phosphatidyl oxygens indicates that the observation of hydrogen bonding in longer time scales might raise these peaks as compared with the peak of $O1_P$. Around the OH group, the $O1_P$ gives the strongest peak too, but here, in addition, the $O3_P$ and $O4_P$ are relatively significant. Interestingly, these interactions have been presented as possible explanations for

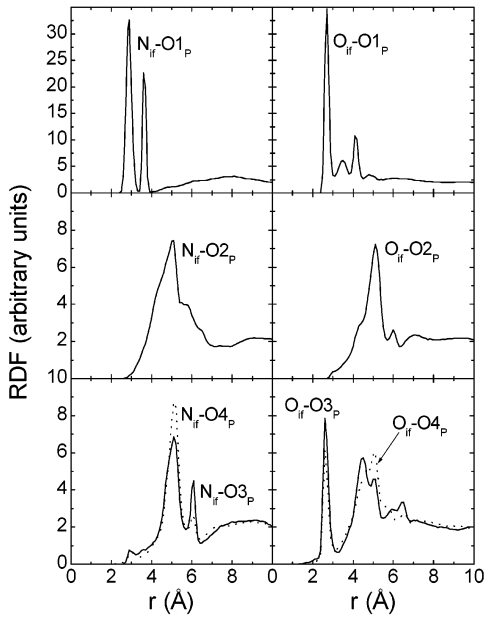

Figure 6. Radial distributions of the phosphoryl oxygens $O1_P$ (upper panels; solid line), $O2_P$ (middle panels; solid line), and $O3_P$ and $O4_P$ (lower panels; solid and dashed line, respectively) around nitrogen (N_{if}, left panels) and oxygen atoms (O_{if}, right panels) of the interfacial region.

the observations by proton NMR.[14] These findings of the possible hydrogen-bonding interactions between the SM molecules imply that the hydrogen bonding between SM and cholesterol molecules would most likely play a role in stabilizing the preferential interaction between them, as suggested in the literature.[3,9]

To describe the ordering of the hydrocarbon chain segments and to be able to make some comparison with the experimental observations for corresponding systems, their order parameters are often calculated from membrane simulations. The deuterium order parameter profiles are shown here in Figure 8. To the best of our knowledge, the deuterium NMR measurements for the sphingomyelin molecules in bilayers are lacking and therefore only a rough comparison with PCs can be made. The order parameters of the DPPC palmitoyl chain in a liquid-crystalline DPPC bilayer and in bovine brain SM bilayer with 5% and 30% cholesterol are shown for comparison[50,51] and reveal that the SM system is significantly more ordered than the liquid-crystalline membranes but not as ordered as systems in which large quantities of cholesterol have been incorporated.[51,52] The order of the chain segments remains high until the end of the chains and the order parameters drop only in their last segments. The first three carbon segments in the SPH chain correspond to the glycerol backbone of the PC molecules and, in principle, the actual chain begins with the trans double

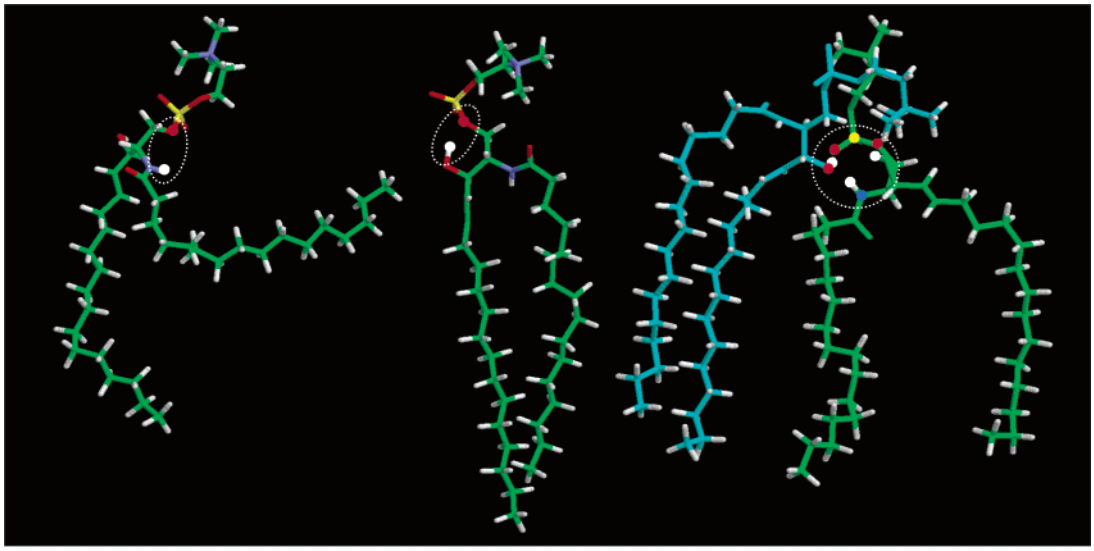

Figure 7. Snapshots of the conformations of 16:0-SM molecules during the simulation, showing the typical close intramolecular arrangement of the NH group and the O1P atom (left), intramolecular hydrogen bonding between the OH group and the O1P atom (middle), and the intermolecular complex formation (right). The coloring is as in Figure 3, except that, to differentiate the other SM molecule in the complex (right), the heavy atoms are colored green in one and cyan in the other SM. However, the color coding of Figure 3 was applied to the small spheres in the positions of interacting atoms.

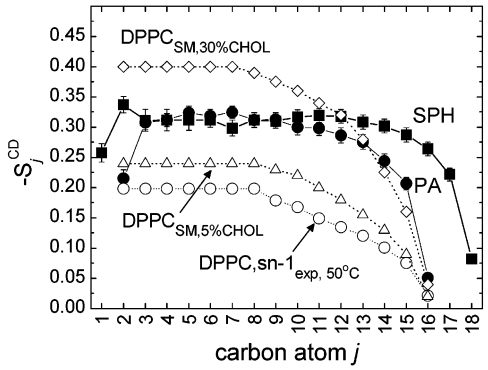

Figure 8. Averages of the $-S_j^{CD}$ orientational order parameters along the SPH and PA chains. The SEMs of the molecular averages are shown as error bars for the values from the simulation. The numbering of the carbon segments is as in Figure 1. For comparison, the experimental deuterium order parameter profiles of the DPPC phosphatidylcholines in a liquid-crystalline phase at 50 °C is given[50] together with DPPC in bovine brain SM system with both 5% and 30% cholesterol at the temperature of 45 °C.[51]

bond between the carbons C4 and C5. The trans conformation of the double bond does not cause any dip in the order parameters, unlike the cis double bonds in the sn-2 chains of PC molecules.[36,53−56] It is in accordance with both the experimental and computational studies that the trans double bonds do not alter the chain behavior as dramatically as do the cis double bonds.[57,58] The lower order parameter value of the carbon C2 of the PA chain indicates the tilted beginning of this chain. The first carbon segments of the fatty acyl chain of the sphingomyelin molecules have been suggested already early on to present similar features as the beginning of the sn-2 chains of PCs,[59] where the tilted conformation has been concluded from both experimental and simulation studies.[36,57] This special behavior of the C2 segment is related to the rotational hindrance of this segment, which results in significant unequivalence between the orientations of its hydrogens and in a difference of 0.11 between the CH_a and CH_b order parameters (data not shown). This kind of unequivalence has been earlier reported from a simulation study of PLPC[60] and in several ^2H NMR studies on sn-2 chains of PCs.[57,61−67] Indeed, the prevailing conformation in the SMs in the simulation is similar to the PCs in that N21 and C1 in the beginning of the PA chains are, on average, at the same height in the bilayer, which affects the orientation of the C2 segment (data not shown).

Conclusions

Despite the intense research over the past few years on the molecular level phenomena in sphingomyelin (SM) containing biological membranes, molecular dynamics (MD) simulation studies on SM have been lacking. Here, the aim was to construct an all-atom bilayer model system of biologically prevailing, palmitoyl chain-containing SMs (16:0-SM), and to determine its characteristics at the molecular level at physiological temperature by MD simulation. The equilibrated 16:0-SM bilayer system shows well the general properties known for this particular SM, namely, the mixed state of the condensed and liquid phases at the temperature just below the condensed-to-liquid transition temperature. The properties of the phosphocholine headgroup were similar to those for phosphatidylcholine (PC) molecules, that is, the phosphorus−nitrogen vector is, on average, roughly parallel to the membrane plane but has large orientational freedom leading to a rough membrane−water interface. The water molecules, again, orient strongly at the surface of the bilayer because of the hydrogen bonding to phosphoryl oxygens, as they do at the surface of PC bilayers. However, the additional NH and OH groups at the interfacial region lead to the extra orientation of water molecules, although now opposite to the effect caused by the phosphoryl oxygens.

When compared to the PCs, the hydrogen-bonding properties of the NH and OH groups make the SMs unique and serve as a basis for direct and water-mediated interactions between the individual SM molecules. In addition, intramolecular hydrogen bonding seems to be of significance between these groups and phosphoryl oxygens. The mixed state of the system leads to relatively ordered hydrocarbon chains. The average order behavior, however, reflects the features of both the very condensed and the still liquidlike conformations of the chains. Altogether, below the transition temperature, the ordering of the molecules is increased and the packing is more efficient, but the properties at the interfacial region and at the headgroups

show considerable motion and disorder. Interestingly, the trans double bond seems not to have such a dramatic effects on chain ordering as its cis counterpart has in PCs.

The compositional variety among the SMs is large as in the PCs. The sphingomyelin species studied here, namely, 16:0-SM, has often been studied experimentally and it is also a physiologically relevant phospholipid. Therefore, it serves as a good starting point for studies of SMs by simulation methods. In the future, it will be interesting to characterize the properties of SM species with long fatty acyl chains, which possibly contain cis monounsaturation in the lower part of their chains. These molecules have been of interest for studies of the special behavior of SMs, like the chain interdigitation and complex phase behavior near physiological temperature.[3] In addition to characterizing the individual SM species, the interaction of SM molecules with other membrane components should also be in the focus of the simulation studies. This work serves as an initial step and basis for development of simulation studies of biological membranes, with the ultimate aid to better understand the functions of membrane domains, such as the rafts, in which sphingolipids are thought to play an essential role.

Acknowledgment. We thank the Center for Scientific Computing (Espoo, Finland) for the computer resources. The Wihuri Research Institute is maintained by the Jenny and Antti Wihuri Foundation. This work was supported by grants from the Federation of Finnish Insurance Companies and the Academy of Finland.

Supporting Information Available: The force field of SM molecules. This material is available free of charge via the Internet at http://pubs.acs.org.

References and Notes

(1) Hannun, Y. A. *J. Biol. Chem.* **1994**, *269*, 3125−3128.
(2) Hauser, J. M. L.; Buehrer, B. M.; Bell, R. M. *J. Biol. Chem.* **1994**, *269*, 6803−6809.
(3) Ramstedt, B.; Slotte, J. P. *FEBS Lett.* **2002**, *531*, 33−37.
(4) Brown, R. E. *J. Cell Sci.* **1998**, *111*, 1−9.
(5) Simons, K.; Ikonen, E. *Science* **2000**, *290*, 1721−1726.
(6) Masserini, M.; Ravasi, D. *Biochim. Biophys. Acta* **2001**, *1532*, 149−161.
(7) Murphy, H. C.; Burns, S. P.; White, J. J.; Bell, J. D.; Iles, R. A. *Biochemistry* **2000**, *39*, 9763−9770.
(8) Hevonoja, T.; Pentikäinen, M. O.; Hyvönen, M. T.; Kovanen, P. T.; Ala-Korpela, M. *Biochim. Biophys. Acta* **2000**, *1488*, 189−210.
(9) Ohvo-Rekilä, H.; Ramstedt, B.; Leppimäki, P.; Slotte, J. P. *Prog. Lipid Res.* **2002**, *41*, 66−97.
(10) Lamba, O. P.; Borchman, D.; Sinha, S. K.; Sundeep, L.; Yappert, M. C.; Lou, M. F. *J. Mol. Struct.* **1991**, *248*, 1−24.
(11) Maulik, P. R.; Shipley, G. G. *Biochemistry* **1996**, *35*, 8025−8034.
(12) Ramstedt, B.; Slotte, J. P. *Biophys. J.* **1999**, *77*, 1498−1506.
(13) Li, X.-M.; Smaby, J. M.; Momsen, M.; Brockman, H. L.; Brown, R. E. *Biophys. J.* **2000**, *78*, 1921−1931.
(14) Talbott, M. C.; Vorobyov, I.; Borchman, D.; Taylor, K. G.; DuPre, D. B.; Yappert, M. C. *Biochim. Biophys. Acta* **2000**, *1467*, 326−337.
(15) Tieleman, D. P.; Marrink, S.-J.; Berendsen, H. J. C. *Biochim. Biophys. Acta* **1997**, *1331*, 235−270.
(16) Tobias, D. J.; Tu, K.; Klein, M. L. *Curr. Opin. Coll. Int. Sci.* **1997**, *2*, 15−26.
(17) Bandyopadhyay, S.; Tarek, M.; Klein, M. L. *Curr. Opin. Coll. Int. Sci.* **1998**, *3*, 242−246.
(18) Forrest, L. R.; Sansom, M. S. P. *Curr. Opin. Struct. Biol.* **2000**, *10*, 174−181.
(19) Feller, S. E. *Curr. Opin. Coll. Int. Sci.* **2000**, *5*, 217−223.
(20) Tobias, D. J. Membrane simulations. In *Computational Biochemistry and Biophysics*; Becker, O. M., MacKerell, A. D., Jr., Roux, B., Watanabe, M., Eds.; Marcel Dekker: New York, Basel, 2001; pp 465−496.
(21) Mombelli, E.; Morris, R.; Taylor, W.; Fraternali, F. *Biophys. J.* **2003**, *84*, 1507−1517.
(22) Ramstedt, B.; Leppimäki, P.; Axberg, M.; Slotte, J. P. *Eur. J. Biochem.* **1999**, *266*, 997−1002.
(23) van Aalten, D. M. F.; Bywater, R.; Findlay, J. B. C.; Hendlich, M.; Hooft, R. W. W.; Vriend, G. *J. Comput.-Aided Mol. Des.* **1996**, *10*, 255−262.
(24) *InsightII User Guide*; MSI: San Diego, CA, MSI, 1995.
(25) Brooks, B. R.; Bruccoleri, R. E.; Olafson, B. D.; States, D. J.; Swaminathan, S.; Karplus, M. *J. Comput. Chem.* **1983**, *4*, 187−217.
(26) Schlenkrich, M.; Brickmann, J.; MacKerell, A. D., Jr.; Karplus, M. An empirical potential energy function for phospholipids: criteria for parameter optimization and applications. In *Biological membranes: a molecular perspective from computation and experiment*; Merz, K. M., Jr., Roux, B., Eds.; Birkhäuser: Boston, MA, 1996; pp 31−81.
(27) Jorgensen, W. L.; Chandrasekhar, L.; Madura, J. D.; Impey, R. W.; Klein, M. L. *J. Chem. Phys.* **1983**, *79*, 926−935.
(28) Darden, T.; York, D.; Pedersen, L. G. *J. Chem. Phys.* **1993**, *98*, 10089−10092.
(29) Essmann, U.; Perera, L.; Berkowitz, M. L.; Darden, T.; Lee, H.; Pedersen, L. G. *J. Chem. Phys.* **1995**, *103*, 8577−8593.
(30) Laaksonen, L. *J. Mol. Graphics* **1992**, *10*, 33−34.
(31) Seelig, J.; Niederberger, W. *J. Am. Chem. Soc.* **1974**, *96*, 2069−2072.
(32) Bruzik, K. S.; Sobon, B.; Salamonczyk, G. M. *Biochemistry* **1990**, *29*, 4017−4021.
(33) Tristam-Nagle, S.; Zhang, R.; Suter, R. M.; Worthington, C. R.; Sun, W.-J.; Nagle, J. F. *Biophys. J.* **1993**, *64*, 1097−1109.
(34) Sun, W.-J.; Suter, R. M.; Knewston, M. A.; Worthington, C. R.; Tristam-Nagle, S.; Zhang, R.; Nagle, J. F. *Phys. Rev. E* **1994**, *49*, 4665−4677.
(35) Venable, R. M.; Brooks, B. R.; Pastor, R. W. *J. Chem. Phys.* **2000**, *112*, 4822−4832.
(36) Hyvönen, M. T.; Rantala, T. T.; Ala-Korpela, M. *Biophys. J.* **1997**, *73*, 2907−2923.
(37) Fettiplace, R.; Haydon, D. A. *Physiol. Rev.* **1980**, *60*, 510−550.
(38) Vaknin, D.; Kelley, M. S.; Ocko, B. M. *J. Chem. Phys.* **2001**, *115*, 7697−7704.
(39) Feller, S. E.; Pastor, M.; Rojnuckarin, A.; Bogusz, S.; Brooks, B. R. *J. Phys. Chem.* **1996**, *100*, 17011−17020.
(40) Essmann, U.; Berkowitz, M. L. *Biophys. J.* **1999**, *76*, 2081−2089.
(41) Shinoda, W.; Shimizu, M.; Okazaki, S. *J. Phys. Chem. B* **1998**, *102*, 6647−6654.
(42) Flewelling, R.; Hubbell, W. *Biophys. J.* **1986**, *49*, 541−552.
(43) Simon, S. A.; McIntosh, T. J. *Proc. Natl. Acad. Sci. U.S.A.* **1989**, *86*, 9263−9267.
(44) Gawrisch, K.; Ruston, D.; Zimmerberg, J.; Parsegian, V. A.; Rand, R. P.; Fuller, N. *Biophys. J.* **1992**, *61*, 1213−1223.
(45) McIntosh, T. J.; Simon, S. A.; Needham, D.; Huang, C. *Biochemistry* **1992**, *31*, 2020−2024.
(46) Akutsu, H.; Nagamori, T. *Biochemistry* **1991**, *30*, 4510−4516.
(47) Alper, H. E.; Bassolino-Klimas, D.; Stouch, T. R. *J. Chem. Phys.* **1993**, *98*, 9798−9807.
(48) Damodaran, K. V.; Merz, K. M., Jr. *Biophys. J.* **1994**, *66*, 1076−1087.
(49) Essmann, U.; Perera, L.; Berkowitz, M. L. *Langmuir* **1995**, *11*, 4519−4531.
(50) Petrache, H. I.; Dodd, S. W.; Brown, M. F. *Biophys. J.* **2000**, *79*, 3172−3192.
(51) Guo, W.; Kurze, T.; Huber, T.; Afdhal, N. H.; Beyer, K.; Hamilton, J. A. *Biophys. J.* **2002**, *83*, 1465−1478.
(52) Smondyrev, A. M.; Berkowitz, M. L. *Biophys. J.* **2000**, *78*, 1672−1680.
(53) Heller, H.; Schaefer, M.; Schulten, K. *J. Phys. Chem.* **1993**, *97*, 8343−8360.
(54) Baenziger, J. E.; Jarrel, H. C.; Hill, R. J.; Smith, I. C. P. *Biochemistry* **1991**, *30*, 894−903.
(55) Seelig, A.; Seelig, J. *Biochemistry* **1977**, *16*, 45−50.
(56) Seelig, J.; Seelig, A. *Q. Rev. Biophys.* **1980**, *13*, 19−61.
(57) Seelig, J.; Waespe-Sarcevic, N. *Biochemistry* **1978**, *17*, 3311−3315.
(58) Rey, A.; Kolinski, A.; Skolnick, J. *J. Chem. Phys.* **1992**, *97*, 1240−1249.
(59) Sundaralingam, M. *Ann. N. Y. Acad. Sci.* **1972**, *195*, 324−355.
(60) Hyvönen, M. T.; Ala-Korpela, M.; Vaara, J.; Rantala, T. T.; Jokisaari, J. *Chem. Phys. Lett.* **1997**, *268*, 55−60.
(61) Seelig, A.; Seelig, J. *Biochim. Biophys. Acta* **1975**, *406*, 1−5.
(62) Haberkorn, R. A.; Griffin, R. G.; Meadows, M. D.; Oldfield, E. *J. Am. Chem. Soc.* **1975**, *99*, 7353−7355.
(63) Engel, A. K.; Cowburn, D. *FEBS Lett.* **1981**, *126*, 169−171.
(64) Douliez, J.-P.; Leonard, A.; Dufourc, E. J. *Biophys. J.* **1995**, *68*, 1727−1739.
(65) Seelig, J.; Browning, J. L. *FEBS Lett.* **1978**, *98*, 41−44.
(66) Gally, H. U.; Pluschke, G.; Overath, P.; Seelig, J. *Biochemistry* **1979**, *18*, 5605−5610.
(67) Salmon, A.; Dodd, S. W.; Williams, G. D.; Beach, J. M.; Brown, M. F. *J. Am. Chem. Soc.* **1987**, *109*, 2600−2609.